

Frequency Response of AFM Nano Robot in Liquid by Considering the Effect of Cantilever Dimension and Environmental Parameters

S. Sami, M. Damircheli*, M. H. Korayem

Department of Mechanical and Aerospace Engineering,
Science and Research Branch, Islamic Azad University, Tehran, Iran
E-mail: mehrnooshdamircheli@gmail.com

*Corresponding author

Received: 16 April 2014, Revised: 5 June 2014, Accepted: 12 October 2014

Abstract: Dynamic analysis and study of atomic force microscopy in liquid environment are the main goal of this research. Hydrodynamic and squeeze forces act on cantilever of atomic force microscopy which works in liquid environment as well. The present paper investigates the effect of different environmental and physical factors on frequency response diagrams. The frequency response analysis studies the occurrence possibility of a phenomenon which causes disturbance and decreases accuracy of imaging. Timoshenko beam model and finite element method were used to be simulated. Meanwhile, the interaction forces between sample and tip point in gas and liquid environments were also considered in simulations. Achieved results showed that in comparison with gas, resonance frequency decreases considerably in liquid environment which is due to additional mass of liquid and also amplitude decreases in liquid environment for additional damping due to presence of liquid. Meanwhile, several studies in repulsion and attraction area with more and less distance from equilibrium distance, showed that in repulsion state, stimulation frequency is more than attraction area; the reason is related to more hardness in repulsion area, and also the presence of interaction forces revealed the fact that the amplitude is not zero in zero excitation frequency.

Keywords: Atomic Force Microscope, Frequency Response, Hydrodynamic Force, Interaction Forces, Timoshenko Beam, Liquid Environment

Reference: Sami, S., Damircheli, M., and Korayem, M. H., "Frequency Response of AFM Nano Robot in Liquid by Considering the Effect of Cantilever Dimension and Environmental Parameters", Int J of Advanced Design and Manufacturing Technology, Vol. 7/ No. 4, 2014, pp. 55-66.

Biographical notes: S. Sami received his MSc in Mechanical Engineering from Science and Research Branch, Islamic Azad University, Tehran, Iran, in 2014. His current research interest includes modeling, simulation, and Nano robotics. Mehrnoosh Damircheli received her PhD in Mechanical Engineering from Science and Research Branch, Islamic Azad University, Tehran, Iran, in 2014. She is currently assistant professor at the Department of Mechanical Engineering, Shahr-e-Qods Branch, Islamic Azad University, Tehran, Iran. Her current research interest includes dynamic analysis, simulation, vibration analysis, control, finite element analysis and nano robotics. M. Habibnejad Korayem received his BSc and MSc in Mech. Eng. from Amir kabir Univ. of Tech. in 1985 and 1987, respectively. He obtained his PhD in Mech. Eng. from the Univ. of Wollongong, Australia, in 1994. He is a Professor in Mech. Eng. at Iran Univ. of Science and Tech.

1 INTRODUCTION

Atomic force microscopy (AFM) is made of a flexible cantilever with a sharp tip placed at the end of cantilever as the most important part of AFM. When the tip moves onto the sample, it makes some forces on it, bending the cantilever and causing the way of laser beam to change and its reflection to be displaced on detector, producing the topography of surface accordingly. Here, the cantilever had stimulated in a stable frequency that usually is resonance frequency or close to it. The micro cantilever that used in AFM is the essential part and central core of AFM because of its application. Therefore, it is necessary to study the dynamic response and control of micro cantilever in order to reach optimum function.

Optimizing the AFM system, not only leads to increase in sampling speed and accuracy, but also provides higher image resolution and improves the cognition of nano world in a better and more accurate way. Additionally, it enables to access world of nano by making some changes in place of particles, or nano manipulation. Using more accurate dynamic models helps to analyze the response of system in a more efficient way, facilitating the anticipation possibility of its behavior and thus, providing higher possibility of controlling system response. Researchers and creators of AFM device need to know the system behavior, way of imaging, efficient response factors, control improvement, and force measurement in nano scale; this reveals the need to analyze the atomic force microscopy dynamically as an essential issue.

Using silicon cantilever, Putman et al. extracted experimental diagrams in liquid and also proceeded to dynamic analysis in tapping mode [1]. Also, it can be mentioned that Christov [2] has made vast researches concerning interaction forces, while Grass [3] worked on DLVO theory. However hydrodynamic force has been investigated by Vinogradova and Bonaccorso [4]. Bonaccorso et al. reviewed all experimental works done in Newton and non-Newton liquid by using AFM [5]. In recent years, solubility force is studied by Han et al., [6]. Also, Hansma et al. used tapping model that in modeling and simulation and in their case sample excited to movement [7]. H. Korayem et al., has analyzed the control of this nano robot in contact mode during the manipulation [8].

Burnham et al. accessed to curves of probe coming close to sample by using mass-spring model [9] which had some limitations, namely unable to predict the behavior of higher modes. The results of their investigation in air were consistent well with the experimental findings, but their results in liquid could not demonstrate the unsymmetrical amplitude changes in the tapping region. The possible reasons for this discrepancy include an inaccurate point-mass model,

which was discussed above, and the fact that the hydrodynamic force exerted on a cantilever may not be well represented by the drag force on a sphere. Basak et al. studied modified hydrodynamic force by using three dimensional models and then compared its results with those of experimental works [10]. Sang and Bhushan used Euler-Bernoulli theory and simulated AFM cantilever dynamic by finite element method [11]. Habibnejad and Ebrahimi achieved cantilever frequency response by Euler-Bernoulli beam model in liquid environment and have used forward-time simulation method [12]. Habibnejad and Damircheli have studied cantilever frequency response by Timoshenko beam model, and analyzed the response of AFM in different equilibrium distances which is more accurate than Euler Bernoulli beam [13].

The goal of this paper is studying the effect of different geometrical and environmental factors on dynamic behavior of atomic force microscopy. System analysis was done, accordingly, in liquid environment through changing different geometrical parameters such as length, width, height of cantilever, and by changing environmental conditions such as density and liquid viscosity to design a cantilever, providing the best contrast and resolution in topography and for liquid, respectively. In this article, frequency response diagrams are studied and the effectiveness of different parameters in resonance frequency and stimulation domain are presented. The results demonstrated the effect of interaction forces in liquid environment on dynamic behavior of atomic force microscopy. The results indicated that geometrical parameters affect the frequency response of the system more in a liquid medium than in the air. Since hydrodynamic forces in liquid environments are influenced by cantilever dimensions, a more dimensionally appropriate cantilever design would be necessary for these environments.

Considering the fact that biological samples are made of very soft and sensitive materials, the resonant frequencies should be low and due to limited space in liquid, the amplitude should be in a specified range in order to prevent damages during imaging in tapping mode. By considering the effect of geometrical parameters on frequency response, a proper design of cantilever for biological samples may be achieved.

2 MATHEMATICAL MODELING

2.1. Interaction forces in liquid and vacuum environments

In order to analyze dynamically the AFM cantilever, the forces exerted on cantilever in the mentioned environment need to be known. These forces vary in different distances and act as repulsion and attraction.

Interaction forces are classified as vertical and tangential forces, where according to DMT theory, vertical forces are expressed as follows [14]:

$$F_n(d_n) = \begin{cases} F_{vdW}(d_n) = -\frac{A_H R}{6d_n^2} & d_n \geq a_0 \\ F_{DMT}(d_n) = -\frac{A_H R}{6a_0^2} + \frac{4E^* \sqrt{R}}{3} (a_0 - d_n)^{\frac{3}{2}} & d_n < a_0 \end{cases} \quad (1)$$

But according to HERTZ theory, tangential forces would be as [13]:

$$F_t(d_n) = \begin{cases} 0 & d_n \geq a_0 \\ -8G^* \left(\frac{3Rf_c}{4E^*}\right)^{\frac{1}{3}} \Delta_t & d_n < a_0 \end{cases} \quad (2)$$

$$f_c = \frac{4E^* \sqrt{R}}{3} (a_0 - d_n)^{\frac{3}{2}} \quad (3)$$

$$G^* = \left[\frac{(2 - \nu_t)}{G_t} + \frac{(2 - \nu_s)}{G_s} \right]^{-1} \quad (4)$$

G^* is effective shear module and by above mentioned equations, stiffness in air environment can be described as:

$$\left\{ \begin{aligned} K_{air-n} = -\frac{\partial F_n}{\partial d_n} \Big|_{d_n=d_0} &= \begin{cases} -\frac{A_H R}{3d_0^3} & d_n \geq a_0 \\ 2E^* \sqrt{R} (a_0 - d_0)^{\frac{1}{2}} & d_n < a_0 \end{cases} \\ K_{air-t} = -\frac{\partial F_t}{\partial \Delta_t} \Big|_{\Delta_t=d_0} &= \begin{cases} 0 & d_n \geq a_0 \\ 8G^* \left(\frac{3Rf_c}{4E^*}\right)^{\frac{1}{3}} & d_n < a_0 \end{cases} \end{aligned} \right. \quad (5)$$

In this paper, interaction forces on cantilever in liquid environment are a combination of normal and tangential forces as mentioned in Eq. (1) and Eq. (2). Meanwhile DLVO force including a set of electrostatic repulsion forces and Van der Waals in attraction region [15]:

$$F_{DLVO}(d_n) = \frac{4\pi\lambda_D R}{\epsilon\epsilon_0} \sigma_T \sigma_S e^{-\frac{d_n}{\lambda_D}} - \frac{A_H R}{6d_n^2} \quad (6)$$

First part of the above equation describes electrostatic force that is used for very large distances ($D \gg \lambda_D$) in which the difference between surface potential and

surface charge is negligible, and the second part illustrates Van der Waals force for flat surface and spherical tip. Finally, interaction model between spherical tip and flat surface sample has been described as follows which is a set of DLVO and DMT forces.

$$F_{liq-n}(d_n) = \begin{cases} F_{DLVO}(d_n) = \frac{4\pi\lambda_D R}{\epsilon\epsilon_0} \sigma_T \sigma_S e^{-\frac{d_n}{\lambda_D}} - \frac{A_H R}{6d_n^2} & d_n \geq a_0 \\ F_{DMT}(d_n) = \frac{4E^* \sqrt{R}}{3} (a_0 - d_n)^{\frac{3}{2}} + F_{DLVO}(a_0) & d_n < a_0 \end{cases} \quad (7)$$

In above mentioned equations σ_S and σ_T are surface charge density of sample and tip, respectively. a_0 is intermolecular distance of cantilever from sample surface, E^* is the effective elasticity, ϵ is the dielectric constant of medium, ϵ_0 is the vacuum permittivity, A_H is the Hamaker constant, d is the equilibrium distance and R is the sphere radius. $A_H = \pi^2 C_{p_1 p_2}$ is the potential constant of atom-atom set and p_1 and p_2 are the number of atoms in each unit of volume [16]. Stiffness coefficient for interaction force of cantilever in liquid environment is described as follows:

$$\left\{ \begin{aligned} K_{liquid-n} = -\frac{\partial F_n}{\partial d_n} \Big|_{d_n=d_0} &= \begin{cases} \frac{4\pi R}{\epsilon\epsilon_0} \sigma_T \sigma_S e^{-\frac{d_0}{\lambda_D}} - \frac{A_H R}{3d_0^3} & d_n \geq a_0 \\ 2E^* \sqrt{R} (a_0 - d_0)^{\frac{1}{2}} & d_n < a_0 \end{cases} \\ K_{liquid-t} = -\frac{\partial F_t}{\partial \Delta_t} \Big|_{\Delta_t=d_0} &= \begin{cases} 0 & d_n \geq a_0 \\ 8G^* \left(\frac{3Rf_c}{4E^*}\right)^{\frac{1}{3}} & d_n < a_0 \end{cases} \end{aligned} \right. \quad (8)$$

When atoms are put together, at first attract each other very weakly. This attraction increases till atoms come close to each other in a way that their electron cloud repulse each other electrostatically. As the distance between two atoms is decreased, electrostatic repulsion neutralizes the attraction forces slowly. When distance between atoms reaches to several angstroms (as one chemical bond), the attraction force reaches to zero. Atoms are in contact with each other when resultant of interaction forces is positive (repulsion). While tip of cantilever press to sample, the probe of cantilever start to bending rather than pushing the sample and it is due to this fact that interaction forces curve have high slope in contact or repulsive region in comparison to attractive region.

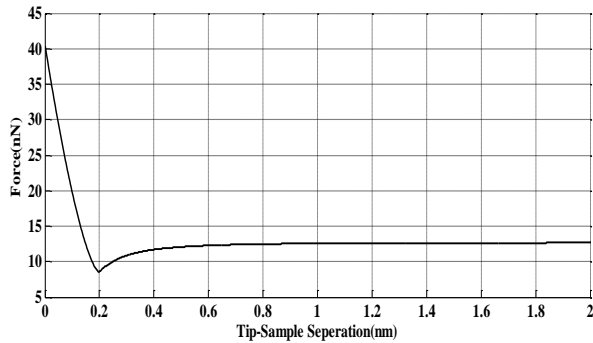


Fig. 1 Force-distance diagram for interaction force

2.2. Forces resulted from liquid

When cantilever immerse in liquid environment, hydrodynamic and squeeze exert on cantilever from the environment. The model that is suggested to describe hydrodynamic force is named “spheres set model”. It means stimulation of beam gets achieved by a set of spheres. The hydrodynamic force that is applied to a sphere floating in a viscose fluid is obtained from the following equation [18]:

$$F_{hyd} = -6\pi\eta R \left(1 + \frac{R}{\delta}\right) \frac{du}{dt} - 3\pi R^2 \sqrt{\frac{2\pi\rho}{\omega}} \left(1 + \frac{2R}{9\delta}\right) \frac{d^2u}{dt^2} \quad (9)$$

Where U is the sphere’s movement, R sphere’s radius, ρ fluid viscosity, ω fluid angular frequency and δ penetration depth $\delta = \sqrt{\frac{2\eta}{\omega\rho}}$.

Table 1 Simulation parameters of interaction force [17]

Parameters	Magnitude
Hamaker constant (A_H)	3.4e-20 j
Debye length (λ_D)	1 μ m
Surface charge density of sample (σ_s)	-0.0025 c/m ²
Surface charge density of tip (σ_T)	-0.032 c/m ²
Dielectric constant of vacuum (ϵ)	8.85e-12 c ² /m ²
Dielectric constant of water (ϵ_0)	80 c ² /m ²
Effective elasticity modulus (E_{eff})	48.7 Gpa
Intermolecular distance (a_0)	0.2E-9 m
Tip radius (R)	10e-9

The hydrodynamic force a apply on a cantilever at a unit length is given by the sum of the forces for spheres in a unit length. Since the number of spheres per unit

length equals $(1/b)$ Where b is width of the beam, then [18]:

$$F_{hyd} = -\left(3\pi\eta + \frac{3}{4}\pi b \sqrt{2\eta\rho_{liq}\omega}\right) \frac{du}{dt} - \left(\frac{1}{12}\pi\rho_{liq}b^2 + \frac{3}{4}\pi b \sqrt{\frac{2\eta\rho_{liq}}{\omega}}\right) \frac{d^2u}{dt^2} \quad (10)$$

Where b is the width of cantilever. According to above equation, the hydrodynamic force is made of two parts:

1. First part is concluded of this fact that fluid has a motion against vibration motion of cantilever which causes damping.

2. The second part of hydrodynamic force by assumption of this fact that some part of fluid have accompanied with cantilever movement and added an additional mass to cantilever. It makes additional mass force that is proportional to acceleration of cantilever.

When cantilever acts near to sample, squeezed film force also is applied to cantilever. By using Reynolds relation, Eq. (11) is derived [19].

$$F_{squeeze} = \frac{\eta b^3}{H(x,t)^3} \frac{du}{dt} \quad (11)$$

Where η is viscosity of the liquid in which the cantilever is immersed, and $H(x,t)$ is the transient distance between cantilever and surface.

$$H(x,t) = D + l \cos \alpha + (L - x) \sin \alpha + u(x,t) \quad (12)$$

Where l is length of probe, D is equilibrium distance between probe and sample surface and L is length of cantilever.

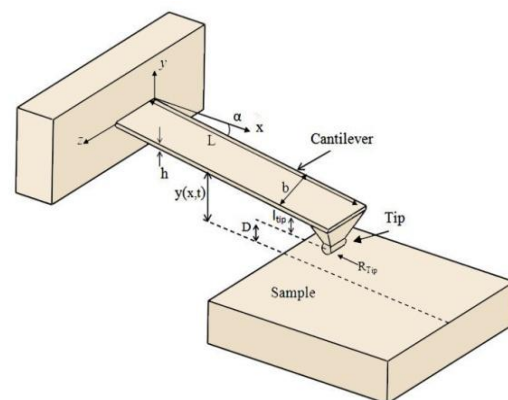


Fig. 2 Schematic view of cantilever, tip and studied sample

2.3. Dynamic modeling of atomic force microscopy cantilever within air and liquid environments

AFM cantilever moves down vertically with a small domain 1-5nm when tip of cantilever processed sample surface by contact method. Therefore, a linear model could have been used to describe interaction forces between tip and sample. As, shown in Fig. 3, AFM cantilever is a small elastic beam with length of L and width of b and thickness of h, which is clamped in one end and the other end free with a conical shape tip. Normally, cantilever makes an angle with sample surface which has been shown by α in fig 2.

Each node of Timoshenko beam element has two degrees of freedom that are vertical and rotational displacements in each node. This model is accurate in comparison to Euler Bernoulli beam model as rotational inertia and shear deformation has been taken into consideration as well. Timoshenko beam equation is as follows:

$$\frac{\partial}{\partial x} \left[KGA \left(\frac{\partial y(x,t)}{\partial x} - \phi(x,t) \right) \right] - c \frac{\partial y(x,t)}{\partial t} - \rho A \frac{\partial^2 y(x,t)}{\partial t^2} + f_h(x,t) = 0$$

$$\frac{\partial}{\partial x} \left(EI \frac{\partial \phi(x,t)}{\partial x} \right) + KGA \left(\frac{\partial y(x,t)}{\partial x} - \phi(x,t) \right) - \rho I \frac{\partial^2 \phi(x,t)}{\partial t^2} = 0 \quad (13)$$

Where $K, G, A, y(x,t), \phi(x,t), \rho, I, E, c$ and $f_h(x,t)$ are the shear coefficient, shear modulus, area of cross section, transverse deflection of beam, bending angle of beam, mass density of beam, moment of inertia of cross section, Young's modulus, internal damping of cantilever and the hydrodynamic force exerted on cantilever by the liquid environment, respectively. The boundary conditions for this cantilever are as follows:

$$y(x,t) = \phi(x,t) = 0 \quad x = 0$$

$$-KGA \left(\frac{\partial y(x,t)}{\partial x} - \phi(x,t) \right) = k_n y(x,t) + c_n \frac{\partial y(x,t)}{\partial t} \quad x = L \quad (14)$$

$$EI \frac{\partial \phi(x,t)}{\partial x} = 0 \quad x = L$$

Stiffness matrix for each element of Timoshenko beam is as follows [13]:

$$[K]_e = \frac{12EI}{L(L^2 + 12\varphi)} \begin{bmatrix} 1 & \frac{L}{2} & -1 & \frac{L}{2} \\ \frac{L}{2} & \frac{L^2}{3} + \varphi & -\frac{L}{2} & \frac{L^2}{6} - \varphi \\ -1 & -\frac{L}{2} & 1 & -\frac{L}{2} \\ \frac{L}{2} & \frac{L^2}{6} - \varphi & -\frac{L}{2} & \frac{L^2}{3} + \varphi \end{bmatrix} \quad (15)$$

In which $\varphi = \frac{EI}{kGA}$, If φ is zero it indicates shear rigidity and stiffness matrix will be in the form of Euler Bernoulli stiffness matrix. Mass matrix must be obtained for each element that follows the first part of the mass matrix due to shear, and the second moment of the mass matrix for the rotational moment [13]:

$$[m]_e = [m_t]_e + [m_r]_e \quad (16)$$

Damping matrix is as following:

$$C_{diagonal} = \begin{bmatrix} \frac{\omega_1}{Q_1} & 0 & 0 & \dots \\ 0 & \frac{\omega_2}{Q_2} & 0 & 0 \\ 0 & 0 & \frac{\omega_3}{Q_3} & 0 \\ \vdots & 0 & 0 & \ddots \end{bmatrix} \quad (17)$$

And finally, non-diagonal damping matrix has been achieved as:

$$C = (\Phi^T)^{-1} C_{diagonal} (\Phi)^{-1} \quad (18)$$

Final equation of limited elements is as following:

$$[M] \{\ddot{u}\} + [C] \{\dot{u}\} + [K] \{u\} = \{F_e\} \quad (19)$$

Where $\{F_e\}$ is excitation force that is entered to cantilever; and $[M], [C]$ and $[K]$ are mass, damping and stiffness matrices, respectively. Acoustic stimulation for cantilever is as follows [20]:

$$u(x,t) = d(x,t) + Jg(t) \quad (20)$$

Where $u(x,t)$ is total displacement, $g(t)$ is harmonic stimulation and J is location vector of cantilever whose quantity is one if there is a displacement in element, otherwise, it is zero. Harmonic stimulation is as the following:

$$g(t) = A \sin(\omega t) \quad (21)$$

Where A is the stimulation amplitude and ω is the stimulation frequency of cantilever. By inserting Eq.

(21) into Eq. (19), the general equation for air and fluid environments is as follows:

$$[M] \ddot{d} + [C] \dot{d} + [K] d = \{F_e\} - [M] J \ddot{g} \quad (22)$$

$$([M] + [M_{add}]) \ddot{d} + ([C] + [C_{add}]) \dot{d} + [K] d = \{F_e\} - ([M] + [M_{add}]) J \ddot{g} - [C_{add}] J \dot{g} \quad (23)$$

Where $[M]$ is the mass matrix, $[C]$ is the damping matrix, and $[K]$ is the stiffness matrix. $[M_{add}]$ is added matrix due to fluid and $[C_{add}]$ is hydrodynamic damping which is achieved by the following relations [18]:

$$M_{add} = \frac{\rho_{add}}{\rho A} M \quad (24)$$

$$C_{add} = \frac{C_{hyd}}{\rho A} M + C_{sq} \quad (25)$$

In which C_{sq} is the squeezed damping that is zero for long distances and ρ_{add} is density of added mass [19]:

$$\rho_{add} = \frac{1}{12} \pi \rho_{liq} b^2 + \frac{3}{4} \pi b \sqrt{\frac{2\eta \rho_{liq}}{\omega}} \quad (26)$$

$$C_{sq} = \int_0^L C_{sq} [N]^T [N] dx = \frac{C_{sq}}{\rho A} m_e \quad (27)$$

$$C_{sq} = \frac{\eta b^3}{h(x,t)^3} \quad (28)$$

Where D is the equilibrium distance between tip and surface. The hydrodynamic damping can be obtained as follows:

$$c_{hyd} = 3\pi\eta + \frac{3}{4} \pi b \sqrt{2\rho_{liq}\eta\omega} \quad (29)$$

Hydrodynamic and squeeze forces have important effects on frequency response. Also, resonant frequency of free cantilever could have been achieved by the following relation in a relative accuracy [20]:

$$\omega_n = \beta_n \sqrt{\frac{EI}{\rho A}} \quad (30)$$

By supposing that $u = Ue^{i\omega t}$, the frequency response equations is achieved as:

$$(K + i\omega C - \omega^2 M)U = MJ\omega^2 \quad (31)$$

$$FRF(\omega)|_{Air} = [K + i\omega C - \omega^2 M]^{-1} [MJ\omega^2] \quad (32)$$

$$FRF(\omega)|_{Liquid} = [K + i\omega(C + C_{add}) - \omega^2(M + M_{add})]^{-1} [(M + M_{add})J\omega^2 - i\omega(C_{add})J] \quad (33)$$

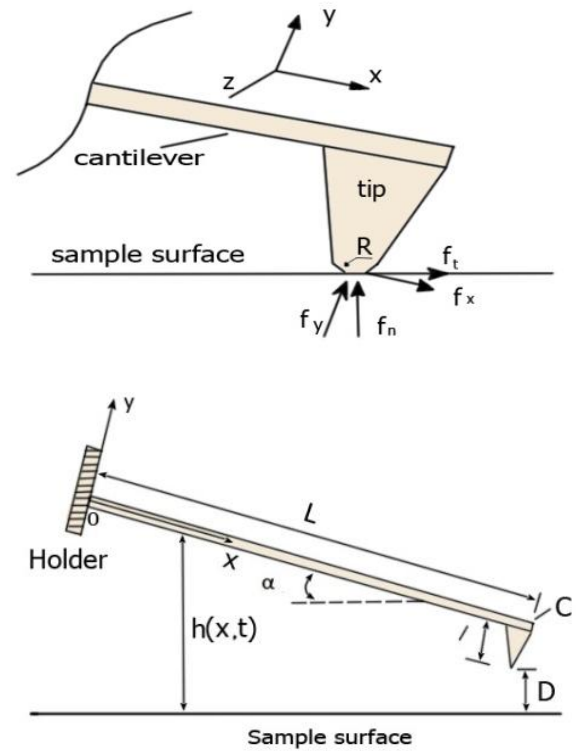


Fig. 3 Parameters and forces on tip of the cantilever

Considering Fig. 3 and linearizing these equations in very small domains, the following equations are gained:

$$\begin{cases} f_n = -K_n \Delta_n \\ f_t = -K_t \Delta_t \end{cases} \quad (34)$$

$$\begin{cases} \Delta_n = u \cos \alpha - l \theta \sin \alpha \\ \Delta_t = l \theta \cos \alpha + u \sin \alpha \end{cases} \quad (35)$$

Where K_n and K_t are lateral and vertical contact stiffnesses, respectively. Considering Fig. 3, force and torque in the last element are as follows:

$$\begin{aligned} f_y &= f_t \sin \alpha + f_n \cos \alpha \\ M_z &= l(f_t \cos \alpha - f_n \sin \alpha) \end{aligned} \quad (36)$$

$$F_{t-s} = -K_{t-s} u \longrightarrow \begin{Bmatrix} F_y \\ M_z \end{Bmatrix} = -[K_{t-s}] \begin{Bmatrix} y \\ \theta \end{Bmatrix} \quad (37)$$

$$K_{t-s} = \begin{bmatrix} K_n \cos^2 \alpha + K_t \sin^2 \alpha & l \cos \alpha \sin \alpha (K_t - K_n) \\ l \cos \alpha \sin \alpha (K_t - K_n) & l^2 (K_t \cos^2 \alpha + K_n \sin^2 \alpha) \end{bmatrix} \quad (38)$$

By inserting Eq. (37) into Eq. (32) and (33), frequency response function is achieved. However, frequency response of cantilever in air is derived as:

$$FRF(\omega)_{Air} = \left[(K + K_{t-s}) + i\omega C - \omega^2 M \right]^{-1} \left[MJ\omega^2 - K_{t-s} J \right] \quad (39)$$

And for state of floating in liquid, considering added mass and added damping to frequency response function, it follows as:

$$\begin{aligned} FRF(\omega)_{Liquid} &= \left[(K + K_{t-s}) + i\omega(C + C_{add}) - \omega^2(M + M_{add}) \right]^{-1} \\ &\left[(M + M_{add})J\omega^2 - i\omega(C_{add})J - K_{t-s}J \right] \end{aligned} \quad (40)$$

Where M and K are mass and stiffness matrices.

3 DYNAMIC SIMULATION RESULTS

Results of the recent studies have shown that resonance amplitude and frequency decrease in liquid environment, and severity of these changes increases by considering cantilever distance from sample surface, where it may also be in contact with the tip length. It was also observed that nonlinear behavior of the system is improved in liquid environment [21]. The application of atomic force microscopy in liquid environment needs imaging and manipulation of biologic samples. Atomic force microscopy was changed to a necessary device in biology, because it provides imaging and studying mechanical characteristics of biologic samples such as biopolymers and viruses under physiologic

condition (liquid environment) [21]. Micro-cantilever frequency response of atomic force microscopy was achieved according to the parameters of the tables 1, 2 & 3. The effects of geometrical and environmental parameters on frequency response in liquid environment (water) have also been studied.

Table 2 AFM condition data, done by MATLAB software [22]

Parameters	Magnitude
Cantilever length (L)	252 μm
Cantilever width (b)	35 μm
Cantilever thickness (h)	2.3 μm
Cantilever mass density (ρ)	2330 Kg/m ³
Water density (ρ _{water})	1000 kg/m ³
Water viscosity (η _{water})	8.54e-4kg/m.s
Effective elasticity modulus (E*)	10.2 GPa
Effective shear modulus (G*)	4.2 GPa
Elasticity modulus Beam (E)	130 GPa
Poisson's ratio Beam (ν)	0.28
Tip length (l)	10 μm
Tip Radius (r)	10 ηm
Intermolecular distance (a ₀)	0.38 ηm
Hamaker constant in Air (A _{H-Air})	2.96e-20 J
Hamaker constant in water (A _{H-W})	2.96e-19 J
First and second quality factors	33.3
3 th - n th quality factors	0.5

Table 3 Density and viscosity of some fluids in 27^oC

Fluid	(kg/m.s)η	ρ(kg/m ³)
Acetone	3.08e-4	785
CCl ₄	8.79e-4	1590
Butanol	2.47e-3	805

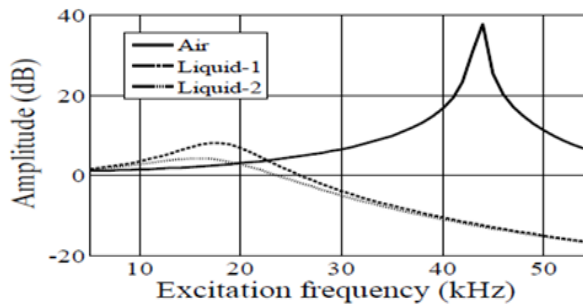
3.1. Comparing diagram of frequency response in liquid and air environments

Fig. 4(a) shows frequency response in both air and liquid environment without applying interaction force, and as expected, the resonance frequency in liquid environment in comparison with air should occur in smaller frequencies. According to the diagrams, the resonance frequency in air is 43.7 KHz, but in liquid environment this frequency is 18 KHz in the first mode. As a result, in liquid environments, the resonance was in lower frequencies and with smaller amplitude. Frequency decrease in liquid caused by additional mass results from liquid, and also decrease of cantilever amplitude occurred due to the damping results from liquid. Comparison of graph 4(a) with graph 4(b) shows that these results have been along with those of the previous research [23].

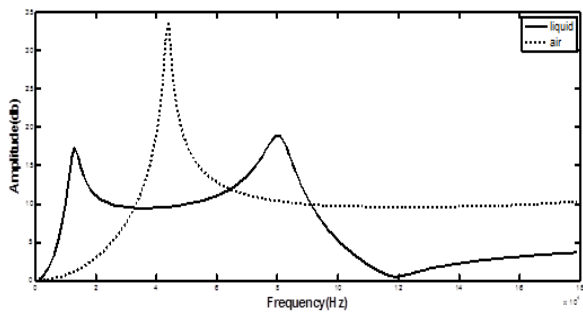
3.2. Effect of density on frequency response

In Fig. 5 the effect of liquid density was studied in frequency response; as expected frequency decreased

by increasing density that is due to increasing added mass. In fact, increase in density causes a rise in the added density (Eq. (26)) and as a result mass rise increases which decreases frequency consequently. Figures 5(a) and 5(b) show the effect of density in presence of interaction forces in attractive and repulsive regions that according to expectations causes frequency to decrease by increasing density.

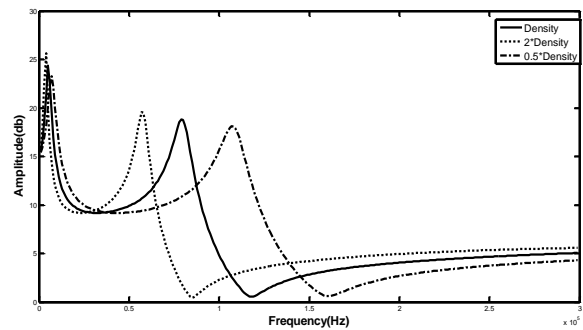


(a)

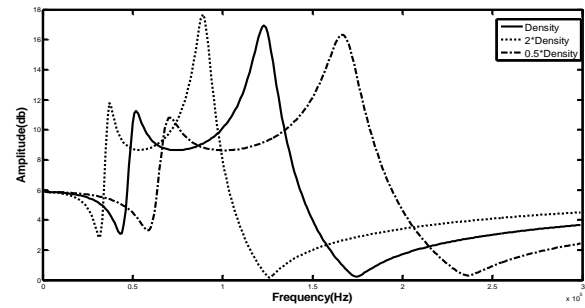


(b)

Fig. 4 Frequency response diagram without applying interaction forces in liquid (a) air results [23], (b) simulation results



(a)

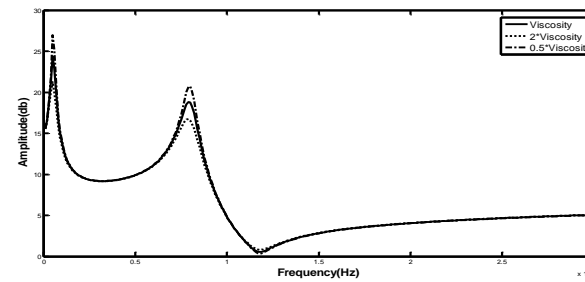


(b)

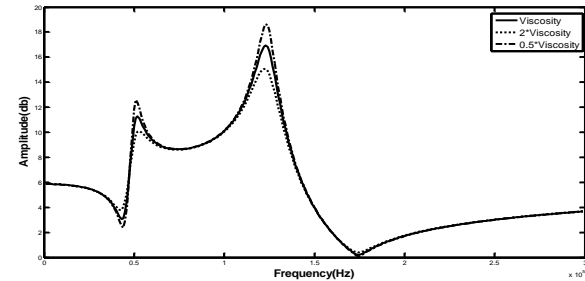
Fig. 5 Effect of fluid density on amplitude-frequency diagrams with Timoshenko beam model considering interaction forces in (a) attractive region, (b) repulsive region

3.3. Effect of viscosity on frequency response

According to Eqs. (28) and (29), damping of squeezed film and hydrodynamic forces increases by increasing viscosity, and as a result, the amplitude should be decreased. In Fig. 6 it is observed that by dividing and then doubling viscosity, the amplitude is increased and decreased, respectively. But it does not have any effect on mass, therefore, frequency remains constant and graphs do not show any change in resonant frequencies.

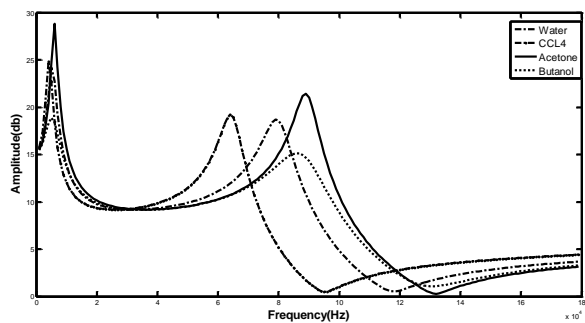


(a)

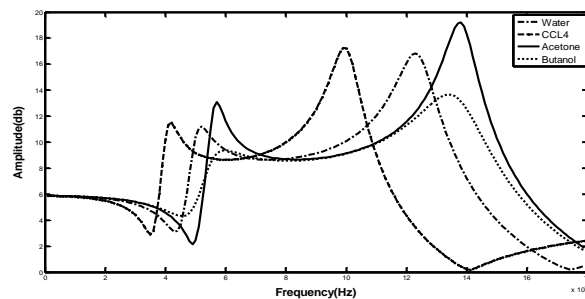


(b)

Fig. 6 Effect of fluid viscosity on amplitude-frequency diagrams by Timoshenko beam model considering interaction forces in (a) attractive region, (b) repulsive region



(a)



(b)

Fig. 7 Frequency response for different liquids with Timoshenko beam model in liquid environment in (a) attractive area, (b) repulsion area

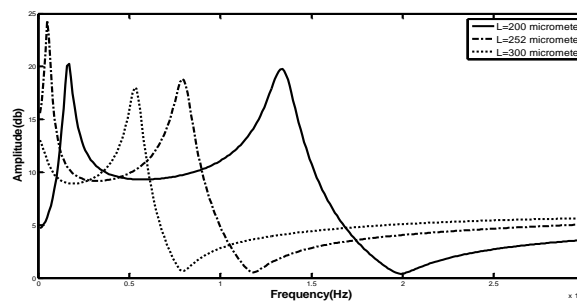
As have been distinguished from Figures 6(a) and 6(b), by increasing fluid viscosity, cantilever vibrating amplitude decreases. The reason is increase of fluid damping coefficient along with viscosity rise. And, also frequency is smaller in attractive region because of lower hardness, and resonance frequency is higher due to rising of cantilever stiffness.

3.4. Frequency response in different liquids

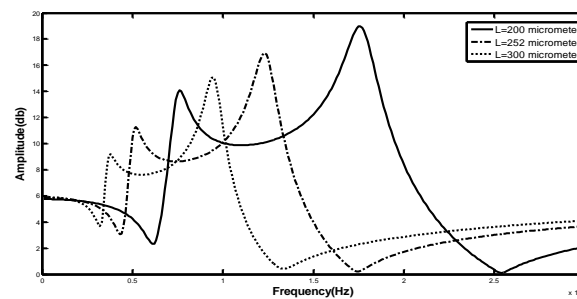
Figure 7 shows frequency response in different liquids with different densities and viscosities according to table (2). According to diagrams in liquids in which density and viscosity increase, the viscosity leaves more significant effect than density on changing amplitude, and increasing viscosity causes amplitude to decrease, but density affects frequency, and frequency decreases while density increases.

3.5. The effect of length of cantilever

Fig. 8 shows frequency response of cantilever of atomic force microscopy with different lengths, and it is observed that increasing length of cantilever decreases resonance frequency as well as the amplitude of response; that is because of decreasing cantilever stiffness according to Eq. (15), increasing cantilever mass, and according to Eq. (16), increase of damping that consequently leads to increasing added mass and squeeze damper which cause resonance frequency and stimulation amplitude to reduce.



(a)



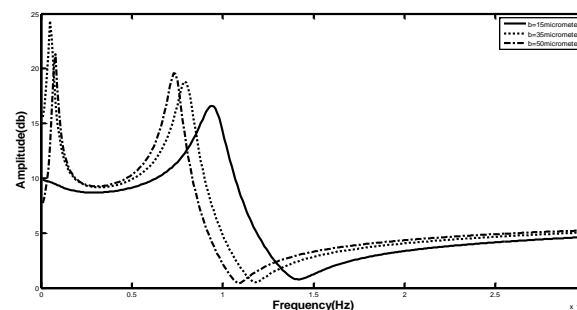
(b)

Fig. 8 Effect of cantilever length on frequency-amplitude diagram with Timoshenko beam model in liquid environment in (a) attractive area, (b) repulsive area

Figures 8(a) and 8(b) show frequency response of cantilever in presence of interaction force which is observed by comparing these two figures in which in attractive area, frequency response occurred in lower frequencies, and in repulsion area these frequencies increased.

3.6. Effect of cantilever width

In Fig. 9 frequency response was achieved with different widths for atomic force microscopy cantilever in which resonance frequency decreased and stimulation amplitude was increased by increasing cantilever width. The reason for frequency decrease could be found in Eq. (26) (added density), because increasing cantilever width caused added density to increase and this density also increases added mass, and as a result frequency decrease was happened.



(a)

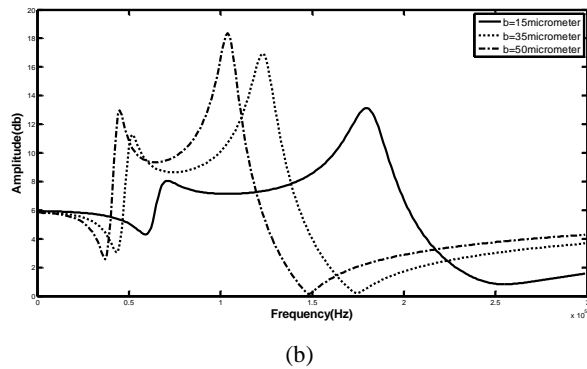


Fig. 9 Effect of cantilever width on frequency- amplitude diagram by Timoshenko beam model in liquid environment (a) attractive area, (b) repulsive area

In figures above, the effect of cantilever width was studied in presence of interaction force which has been occurred by increasing cantilever width, increasing amplitude and decreasing frequency and also in repulsion area it has been increased more because of different force formula in these two areas.

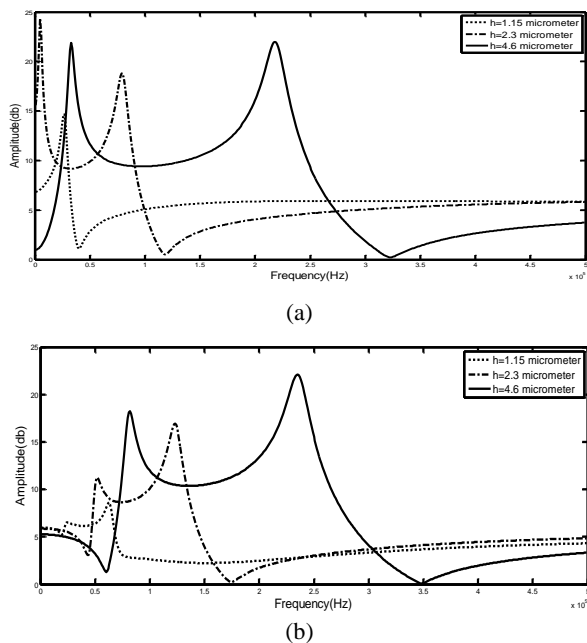


Fig. 10 Cantilever height effect on amplitude-frequency diagrams with Timoshenko beam model by considering interaction forces on frequency in (a) attractive area, (b) repulsive area

3.7. Effect of cantilever height

In Fig. 10 the effect of cantilever height was studied, revealing that increasing cantilever height caused stimulation amplitude and frequency to increase. Moreover, sever effect of cantilever height is obvious in diagrams in which it was decreased strongly by height decrease of the second intensification frequency

and this reduction is more than that of the first mode frequency. Therefore, frequency changes in above modes are more sensible. This frequency and amplitude stimulation increase is due to increasing cantilever cross section that consequently leaves opposite effect on mass and added damper relations which causes them to reduce (Eqs. (24) and (25)). Above mentioned figures show cantilever height effect in attractive and repulsion areas in which a rise in cantilever height caused frequency and stimulation amplitude to increase. Also, because of force, stimulation amplitude in zero frequency excitation does not start from zero.

3.8. Comparing attractive and repulsion areas

Frequency response was obtained and compared in both liquid and gas environments in Fig. 11, and as it is clear from diagrams, due to more hardness in repulsion area, resonance frequency in this area moved to higher frequencies, while it is lower in attractive area. This matter is completely observable in liquid environment but in gas, the first frequency in attractive area moved to resonance frequencies lower than zero. Resonance frequency in the first mode in liquid environment and in attractive area is 50 kHz and in repulsion area, it is 55 kHz and in the second mode they are 80 and 125 kHz in attractive and repulsive areas, respectively.

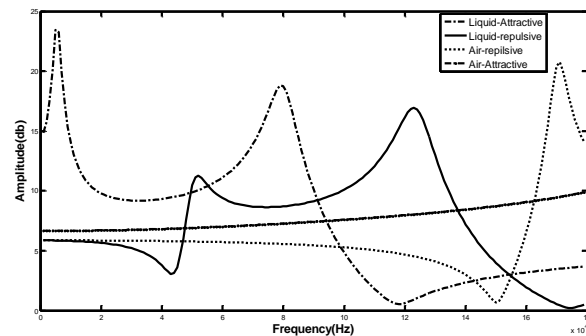


Fig. 11 The frequency response of both air and liquid environments by considering the interactions force of attraction and repulsion area

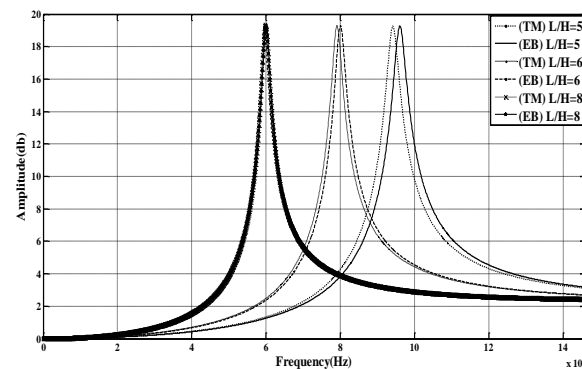


Fig. 12 Comparing frequency response of Euler-Bernoulli and Timoshenko methods [22]

3.9. Comparison of Euler-Bernoulli and Timoshenko methods

And finally, in order to determine the significance and accuracy of the Timoshenko beam model in comparison to Euler-Bernoulli model, the frequency responses of the system for both mentioned models have been investigated by keeping the cantilever length constant and increasing the cantilever thickness. Fig. 12 indicates that by decreasing the length-to-thickness ratio of the cantilever, the difference between the two models becomes so pronounced; and this is another reason for using Timoshenko beam model in the simulations that consider the effects of rotational inertia and shear deformation, especially when using short cantilevers.

4 CONCLUSION

Enjoying wide usage in material topography within vacuum environment, atomic force microscopy has numerous applications in liquid environment, and for biologic materials as well; it can also be used especially in DNA imaging and cancer cells diagnosis. By investigating FRF diagrams it was observed that geometrical parameters have crucial effects on frequency response and it can make some changes on vibration parameters such as resonance frequency, amplitude and phase response due to presence of damping squeeze and hydrodynamic forces. Regarding diagrams in repulsion and attractive areas, it was revealed that in attractive area, resonance frequency is less than repulsion area because of the lower hardness in attractive area in comparison with repulsion.

According to obtained diagrams, reduction in frequency and amplitude were observed while atomic force microscopy cantilever length increased. Similarly vibration amplitude and frequency were increased with the rise of thickness and amplitude and decrease of frequency while cantilever width increased. Also, changing liquid density caused frequency to decrease, and actually, the fluid viscosity rise indicated a decrease in amplitude. Besides, if probe-sample distances (D_0) are bigger than molecular (a_0), forces adopt attractive type and these forces cause resonance frequency to decrease.

According to the presented diagrams, resonance frequency in gas is about 43.7 kHz, while it is 18 kHz in the first mode in liquid. This shows decrease of resonance frequency in liquid which is due to increasing added mass for presence of liquid.

In liquid environment, capillary forces eliminated resulting in decrease in chaotic responses. Also, due to the existence of liquid film on sample, contact forces were decreased that caused a reduction in bi-stability. It was also observed that resonant frequency in liquid

environment was less than in air, and this contributes to avoid damaging gentle biology cells while imaging in liquid.

As a result, by using Timoshenko model, rotational momentum inertia and shear deformation were considered in simulation. In order to increase imaging speed, very useful in studying biologic substances, it seemed necessary to use short beams making it inevitable to use Timoshenko beam model for the accuracy to be improved.

REFERENCES

- [1] Putman, C. A. J., Werf, K. V. D., Grooth, B. G. D., Hulst, N. F. V. and Greve, J., "Tapping Mode Atomic Force Microscopy in Liquid", Applied physics letters, 1994, pp. 2454-2456.
- [2] Nikolay, C., Christov, "Oscillatory Structural Forces Due to Nonionic Surfactant Micelles: Data by Colloidal-Probe AFM vs. Theory", American chemical society, 2009, pp. 915-923.
- [3] Grass, J.D, "A Review of Non-DLVO Interactions in Environmental Colloidal Systems", Re/Views in Environmental Science & Bio/ Technology, 2002, pp. 17-38.
- [4] Bonaccorso, E., Butt, H. J., and Craig, V. S. J., "Surface Roughness and Hydrodynamic Boundary Slip of a Newtonian Fluid in a Completely Wetting System", Phys. Rev.Lett., 2003, pp. 144501(4).
- [5] Bonaccorso, E., Kappl, M., and Butt, H. J., "Thin Liquid Films Studied by Atomic Force Microscopy", Current Opinion in Colloid & Interface Science, Vol. 13, 2008, PP. 107-119.
- [6] Han, W., Lindsay, S. M., "Probing Molecular Ordering at a Liquid- Solid Interface with a Magnetically Oscillated Atomic Force Microscope", App. Phys. Lett., 1998, pp. 1656-1658.
- [7] Hansma, P. K., Cleveland, J. P., and Radmacher, M., "Tapping Mode Atomic Force Microscopy in Liquid," Appl. Phys. Lett., Vol. 64, No. 13, 1994, pp. 1738-1740.
- [8] Korayem, M. H., Noroozi, M., and Daeinabi, K., "Sliding Mode Control of AFM in Contact Mode during Manipulation of Nano-Particle", International Journal of Advanced Design & Manufacturing Technology, Vol. 6, No. 4, 2013.
- [9] Burnham, N. A., Behrendy, O. P., Oulevey, F., and Gremaudy, G., "How Does a Tip Tap?", Nanotechnology, 1997, pp.67-75.
- [10] Basak, S., Raman, A., and Sachs, F., "Hydrodynamics of Torsional Probes for Atomic Force Microscopy in Liquids", Journal of Appl. Phys. Lett., Vol. 102, 2007.
- [11] Song, Y., Bhushan, B., "Finite-Element Vibration Analysis of Tapping-Mode Atomic Force Microscopy in Liquid", Ultramicroscopy, Vol. 107 (10-11), 2007, pp. 1095-1104.
- [12] Habibnejad Korayem, M., Ebrahimi, N., "Nonlinear Dynamics of Tapping-Mode Atomic

- Forcemicroscopy in Liquid”, *Journal of Applied Physics*, Vol. 109, No. 8, 2011, pp. 084301-8.
- [13] Habibnejad Korayem, M., Damircheli, M., “The Effect of Fluid Properties and Geometrical Parameters of Cantilever on the Frequency Response of Atomic Force Microscopy”, *Precision Engineering*, Vol. 38, No. 2, 2013, pp 321-329.
- [14] Maugis, D., “Adhesion of Spheres: the JKR-DMT Transition using a Dugdale Model”, *Journal of Colloid and Interface Science*, 1992, pp.169-243.
- [15] Derjaguin, B., Landau, L., “Theory of the Stability of Strongly Charged Lyophobic Sols and of the Adhesion of Strongly Charged Particles in Solutions of Electrolytes”, *Acta Physico Chemica URSS* . Vol. 14, 1941, pp. 633.
- [16] Butt, H. J., Cappell, B., and Kappl, M., “Force Measurements with the Atomic Force Microscope: Technique, Interpretation and Applications”, *Surface Science Reports*, Vol. 59, 2005, pp 1-152.
- [17] Domke, J., Parak, W. J., George, M., Gaub, H. E., and Radmacher, M., “Mapping the Mechanical Pulse of Single Cardiomyocytes with the Atomic Force Microscope”, *European Biophys. J.*, 1999, pp. 179-186.
- [18] Levine, S., “Problems of Stability in Hydrophobic Colloidal Solutions I. on the Interaction of Two Colloidal Metallic Particles. General Discussion and Applications”, *Proceedings of the royal Society of London, Mathematical and Physical Sciences*, 1939, pp. 145-164.
- [19] Hosaka, H., Itao, K., and Kuroda, S., “Damping Characteristics of Beam-Shaped Micro-Oscillators”, *Sensors and Actuators*, Vol. 49, 1995, pp. 87.
- [20] Habibnejad Korayem, M., Jiryaei Sharan, H., and Habibnejad Korayem, A., “Comparison of Frequency Response of Atomic Force Microscopy Cantilevers under Tip-Sample Interaction in Air and Liquids”, *Scientia Iranica*, 2012, pp. 106-112.
- [21] Basak, S., Ramana, A., “Dynamics of Tapping Mode Atomic Force Microscopy in Liquids: Theory and Experiments”, *Applied Physics Letters*, Vol. 91, 2007, pp. 064107.
- [22] Damircheli, M., Habibnejad Korayem, M., “Dynamic Analysis of the AFM by Applying the Timoshenko Beam Theory in the Tapping Mode and Considering the Impact of the Interaction Forces in a Liquid Environment”, *Canadian Journal of Physics*, Vol. 92, No. 999, 2013, pp 1-12.
- [23] Habibnejad Korayem, M., Ebrahimi, N., and Habibnejad Korayem, A., “Modeling and Simulation of Tapping-Mode Atomic Force Microscopy in Liquid”, *Nanoscience and Nanotechnology*, 2011, pp. 14-21.